Extensive evolutionary and functional diversity among mammalian AIM2-like receptors

Rebecca L. Brunette,[1] Janet M. Young,[2] Deborah G. Whitley,[1] Igor E. Brodsky,[3] Harmit S. Malik,[2,4] and Daniel B. Stetson[1]

[1]Department of Immunology, University of Washington School of Medicine, Seattle, WA 98195
[2]Division of Basic Sciences and [4]Howard Hughes Medical Institute, Fred Hutchinson Cancer Research Center, Seattle, WA 98109
[3]Department of Pathobiology, School of Veterinary Medicine, University of Pennsylvania, Philadelphia, PA 19104

Innate immune detection of nucleic acids is important for initiation of antiviral responses. Detection of intracellular DNA activates STING-dependent type I interferons (IFNs) and the ASC-dependent inflammasome. Certain members of the AIM2-like receptor (ALR) gene family contribute to each of these pathways, but most ALRs remain uncharacterized. Here, we identify five novel murine ALRs and perform a phylogenetic analysis of mammalian ALRs, revealing a remarkable diversification of these receptors among mammals. We characterize the expression, localization, and functions of the murine and human ALRs and identify novel activators of STING-dependent IFNs and the ASC-dependent inflammasome. These findings validate ALRs as key activators of the antiviral response and provide an evolutionary and functional framework for understanding their roles in innate immunity.

CORRESPONDENCE
Daniel B. Stetson:
stetson@uw.edu

Abbreviations used: ALR, AIM2-like receptor; BMDC, BM-derived DC; BMDM, BM-derived macrophage; HA, hemagglutinin; ISD, IFN-stimulatory DNA; ISRE, IFN-stimulated response element; MEF, murine embryonic fibroblast; TLR, Toll-like receptor.

Innate and adaptive antiviral responses are initiated by detection of nucleic acids. The mammalian sensors of these nucleic acids can be broadly classified into two groups. Toll-like receptors (TLRs) are expressed most prominently by innate immune cells and link detection of nucleic acids within phagosomes to signals that are important for activation of lymphocytes. Additionally, intracellular receptors detect the presence of parasitic nucleic acids derived from viral genomes and invasive bacteria within infected cells. Much progress has been made in understanding the sensors and signaling pathways triggered by these receptors, as well as their essential role in protective immunity and their pathological contribution to certain autoimmune diseases (Barbalat et al., 2011).

All viruses contain a genome made of either RNA or DNA, and accordingly, innate immune sensors for both of these nucleic acids are broadly expressed in mammalian cells to detect infection. The RIG-I and MDA5 RNA helicases are the principal intracellular receptors for viral RNA and signal activation of the type I IFN-mediated antiviral response through the adaptor protein MAVS (Kato et al., 2011). In addition, detection of intracellular DNA activates at least three signaling pathways (Hornung and Latz, 2010). First, the IFN-stimulatory DNA (ISD) pathway is a sequence-independent antiviral response triggered by detection of DNA (Stetson and Medzhitov, 2006) that activates type I IFN gene expression through the adaptor protein STING (Ishikawa and Barber, 2008; Ishikawa et al., 2009). Second, detection of A/T-rich DNA (Ishii et al., 2006) activates the innate immune response through STING (Sharma et al., 2011) and through transcription of this DNA by cellular RNA polymerase III (Pol III) into RNA that activates the RIG-I pathway (Ablasser et al., 2009; Chiu et al., 2009). Interestingly, cyclic dinucleotides that act as second messengers in bacteria trigger STING activation through direct binding to STING itself (Burdette et al., 2011; Sauer et al., 2011). Finally, intracellular DNA activates the inflammasome (Muruve et al., 2008), an ASC/caspase-1–dependent signaling complex that mediates processing

The Rockefeller University Press $30.00
J. Exp. Med. 2012 Vol. 209 No. 11 1969-1983
www.jem.org/cgi/doi/10.1084/jem.20121960

The Journal of Experimental Medicine

and secretion of the cytokine IL-1β and a proinflammatory form of cell death called pyroptosis (Strowig et al., 2012).

Identifying the receptors that trigger these pathways has been the subject of intense research. In the case of the RNA Pol III–RIG-I pathway and cyclic dinucleotide sensing, the mechanisms of detection are known (Ablasser et al., 2009; Chiu et al., 2009; Burdette et al., 2011), although the roles of these pathways in host defense remain to be established. AIM2 was recently identified as a key activator of the ASC inflammasome (Bürckstümmer et al., 2009; Fernandes-Alnemri et al., 2009; Hornung et al., 2009; Roberts et al., 2009), and AIM2-deficient mice validate its role in IL-1β production and pyroptosis in response to numerous viruses and intracellular bacteria (Fernandes-Alnemri et al., 2010; Jones et al., 2010; Rathinam et al., 2010). Numerous receptors for the STING-dependent ISD pathway have been proposed, including DAI/ZBP-1 (Takaoka et al., 2007) and DDX41 in DCs (Zhang et al., 2011). However, DAI-deficient mice have a normal ISD pathway (Ishii et al., 2008), and the role of DDX41 in other cell types is unknown. Recently, the AIM2-like receptors (ALRs) human IFI16/mouse IFI204 were implicated in the STING-dependent IFN response (Unterholzner et al., 2010), and IFI16 was also shown to activate the inflammasome in response to Kaposi's sarcoma herpes virus (Kerur et al., 2011). Some of the differences in results in these studies may reflect the use of different activating ligands and various primary and immortalized cell types, thus necessitating a clear definition of STING-activating ligands. Despite the lack of clarity in defining the ISD sensors, it is becoming clear that the STING-dependent ISD pathway is required for the IFN response to numerous DNA viruses (Ishikawa et al., 2009), retroelements and retroviruses (Stetson et al., 2008;Yan et al., 2010), intracellular bacteria (Ishikawa et al., 2009), and parasites (Sharma et al., 2011). Moreover, chronic activation of the ISD pathway has been implicated as the cause of several severe, IFN-associated autoimmune diseases in humans, including Aicardi-Goutieres syndrome (Stetson et al., 2008; Gall et al., 2012).

The recent identification of ALRs that activate the inflammasome (AIM2, IFI16) and the STING-dependent IFN response (IFI16, IFI204) suggests that this family of receptors may play important roles in both pathways. ALRs were first identified as a family of IFN-inducible genes in mice >20 yr ago (Kingsmore et al., 1989; Opdenakker et al., 1989), and most known ALRs contain a Pyrin domain that mediates protein–protein interactions and a HIN domain that can bind directly to DNA (Albrecht et al., 2005; Schattgen and Fitzgerald, 2011), thus making them ideal candidates for innate immune receptors of DNA. Eight ALRs have been previously annotated in mice, and four in humans, but the functions of most of these ALRs remain unknown. Here, we define STING-dependent ligands in multiple cell types, identify five novel ALRs in mice, analyze the phylogeny of mammalian ALRs, and characterize the functions of all known murine and human ALRs. Our analyses reveal functional redundancy among these receptors and extensive evolutionary diversity that is recurrently recreated in mammalian genomes.

RESULTS

Definition of STING-dependent ligands

Numerous ligands have been used to trigger the DNA-activated antiviral response in various cell types, often interchangeably, but the pathways activated by each ligand have not been clearly defined. We therefore performed a comprehensive analysis of these and additional ligands in primary bone-marrow derived macrophages and DCs, and in murine embryonic fibroblasts (MEFs) to directly compare their stimulatory potency and evaluate their requirements for STING and MAVS. Consistent with previous studies (Stetson and Medzhitov, 2006; Ishikawa and Barber, 2008), we found that calf thymus DNA and annealed, 45-bp ISD oligos potently activated IFN-β expression in macrophages and MEFs. This antiviral response was reduced by >99.8% in STING (*Tmem173*)-deficient cells, demonstrating that these two DNA preparations represent pure ISD ligands (Fig. 1 A). As shown previously (McWhirter et al., 2009; Burdette et al., 2011), cyclic di-AMP triggered an IFN-β response that was also entirely STING-dependent (Fig. 1 A). Additionally, we found that the chemotherapeutic agent and nucleoside analogue DMXAA, which activates type I IFN expression (Roberts et al., 2007), is a STING-activating ligand (Fig. 1 A). In contrast, the IFN-stimulating activity of the DNA polymer Poly dA:dT was largely intact in STING-deficient macrophages and MEFs (Fig. 1 A), consistent with its ability to trigger both the ISD pathway and the RNA polymerase III–RIG-I pathway (Ablasser et al., 2009; Chiu et al., 2009). Indeed, the antiviral response to Poly dA:dT was reduced by >99% only in macrophages deficient in both STING and MAVS, and not in macrophages lacking STING alone or MAVS alone (Fig. 1 B). We obtained identical results in BM-derived DCs (BMDCs; Fig. 1 C), demonstrating a substantial redundancy in these cell types between the ISD–STING pathway and the PolIII–RIG-I pathway in response to Poly dA:dT. As expected, an in vitro–transcribed triphosphate RIG-I ligand (Saito et al., 2008) activated MAVS-dependent IFN production, and LPS-induced IFN required neither STING nor MAVS (Fig. 1). Together, these data provide a comparative analysis of IFN-inducing ligands in macrophages, DCs, and MEFs, and genetically define "pure" activators of the STING-dependent antiviral response. Importantly, we formally demonstrate that ISD and Poly dA:dT cannot be used interchangeably as ligands for the DNA-activated antiviral response, and that data implicating specific candidate receptors in the IFN response to Poly dA:dT must be interpreted in light of the two pathways triggered by this polymer (Takaoka et al., 2007; Zhang et al., 2011).

Extraordinary evolutionary diversity among mammalian ALRs

We initiated our analysis of mammalian ALRs by focusing first on ALRs that had been previously annotated in mouse (eight genes) and human (four genes). We also performed an in-depth characterization of the ALR gene family in C57BL/6 mice using homology searches. Our analyses yielded 5 novel genes,

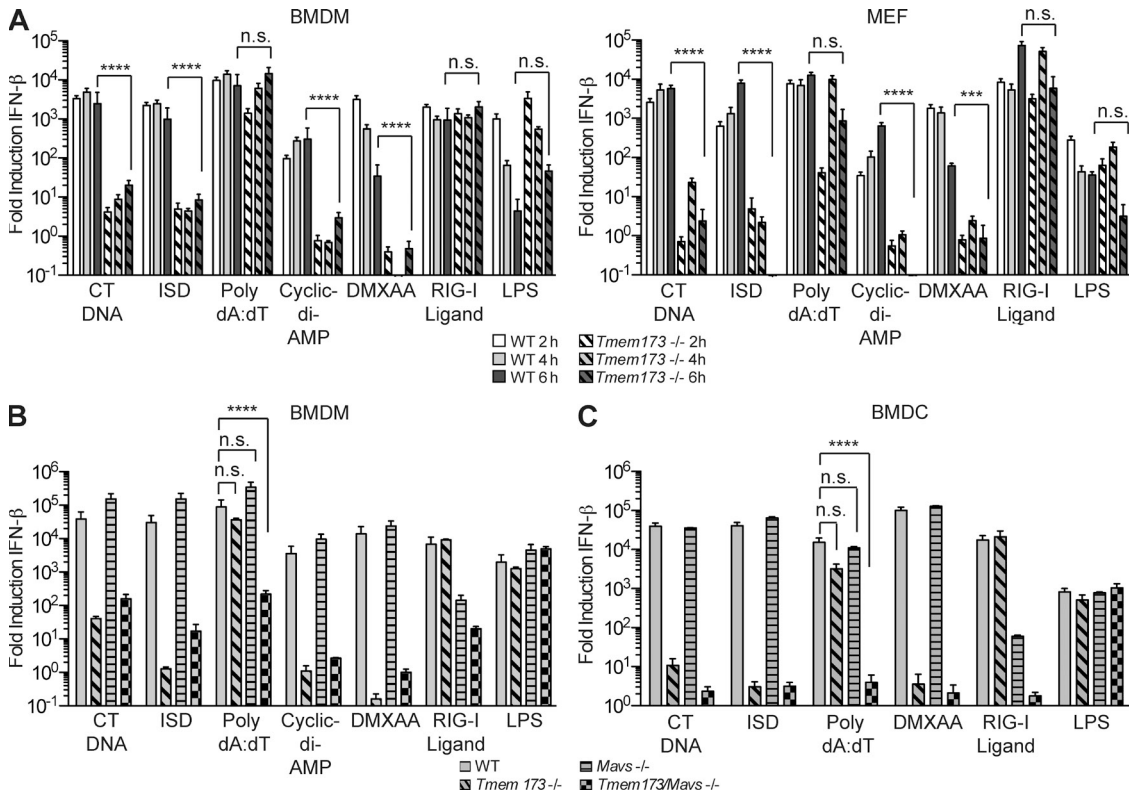

Figure 1. STING is required for sensing of natural DNA, cyclic dinucleotides and DMXAA. (A) Quantitative RT-PCR analysis of IFN-β mRNA expression in WT or *Tmem173*$^{-/-}$ BMDMs (left) and primary, early passage MEFs (right); cells were treated with the indicated ligands and harvested for analysis every 2 h. (B) WT, *Tmem173*$^{-/-}$, *Mavs*$^{-/-}$, and *Tmem173*$^{-/-}$ *Mavs*$^{-/-}$ BMDMs were stimulated with the indicated ligands for 4 h. (C) BMDCs of the indicated genotypes were generated and stimulated with the indicated ligands for 4 h before harvest and quantitative RT-PCR analysis. Data are representative of two to three experiments, each with triplicate treatments for every time point (error bars represent the SEM). Statistical analysis was performed at the 6-h time point (A) and 4-h time point (B and C) with a two-way ANOVA test. ***, $P < 0.001$; ****, $P < 0.0001$; n.s. = not statistically significant ($P > 0.05$). Significant values in panels B and C are identical to those found in Fig. 1 A and are omitted for figure clarity.

bringing the total number of ALR genes within this mouse locus to 13 (Fig. 2 A and Supplemental text). These five newly identified mouse genes are located between the *Aim2* and *Ifi204* genes, and all contain a Pyrin and/or a HIN domain that is diagnostic of the ALR gene family. We named the genes based on domain organization in an effort to distinguish them from the other currently known murine ALRs. The newly identified genes are: *Pyblhin-C*, which contains Pyrin and HIN domains; *Pyhin-B*, which is highly similar to the known *Pyhin-1* open reading frame but has a truncated HIN domain lacking the last 21 aa; *Pyr-A (Pydc4)*, which contains a Pyrin domain but no HIN domain; *Pyr-rv1 (Pydc3)*, which contains a Pyrin domain followed by a three-exon in-frame fusion of three distinct sequences from a murine endogenous retrovirus B2 (ERVB2) open reading frame; and *Pyhin-A*, which contains Pyrin and HIN domains (Fig. 2 A and Supplemental text). Additionally, we found an orphan HIN domain adjacent to the Pyrin domain of *Pyr-rv1* that is most similar to the HIN of *Pyblhin-C*, but we have not yet confirmed that this HIN domain is expressed or linked to the *Pyr-rv1* Pyrin (unpublished data). These five novel genes reveal an even higher complexity within the murine ALR gene family than previously appreciated.

To systematically address the evolutionary underpinnings of the ALR complexity that we have uncovered, we performed genomic characterization of the ALR loci across seven mammalian species that represent ~95 million years of evolutionary divergence. In each of these species, we found a single, continuous ALR locus, flanked by the *Cadm3* gene on one end and by several olfactory receptors and the *Spta1* gene on the other end (Fig. 2 A). Remarkably, the size and makeup of the ALR locus is dramatically different among these species. The murine ALR locus, with 13 genes distributed across 573 kb, is the most expansive among the species we examined (Fig. 2 A). In contrast, horses have six ALR genes, and the rat and human ALR loci each contain four genes. Interestingly, dog and pig each have two ALR genes, and cows only have a single ALR gene (Fig. 2 A). Perhaps the most surprising finding of our analysis is that the canonical inflammasome activator, Aim2, is no longer functional in the cow, sheep, dolphin, pig, cat, and dog genomes because of the acquisition of deletions, frameshifts, and stop codons (Fig. 2, B and C). The shared frameshift mutation between the cow, sheep, and dolphin genomes and the two shared frameshifts between

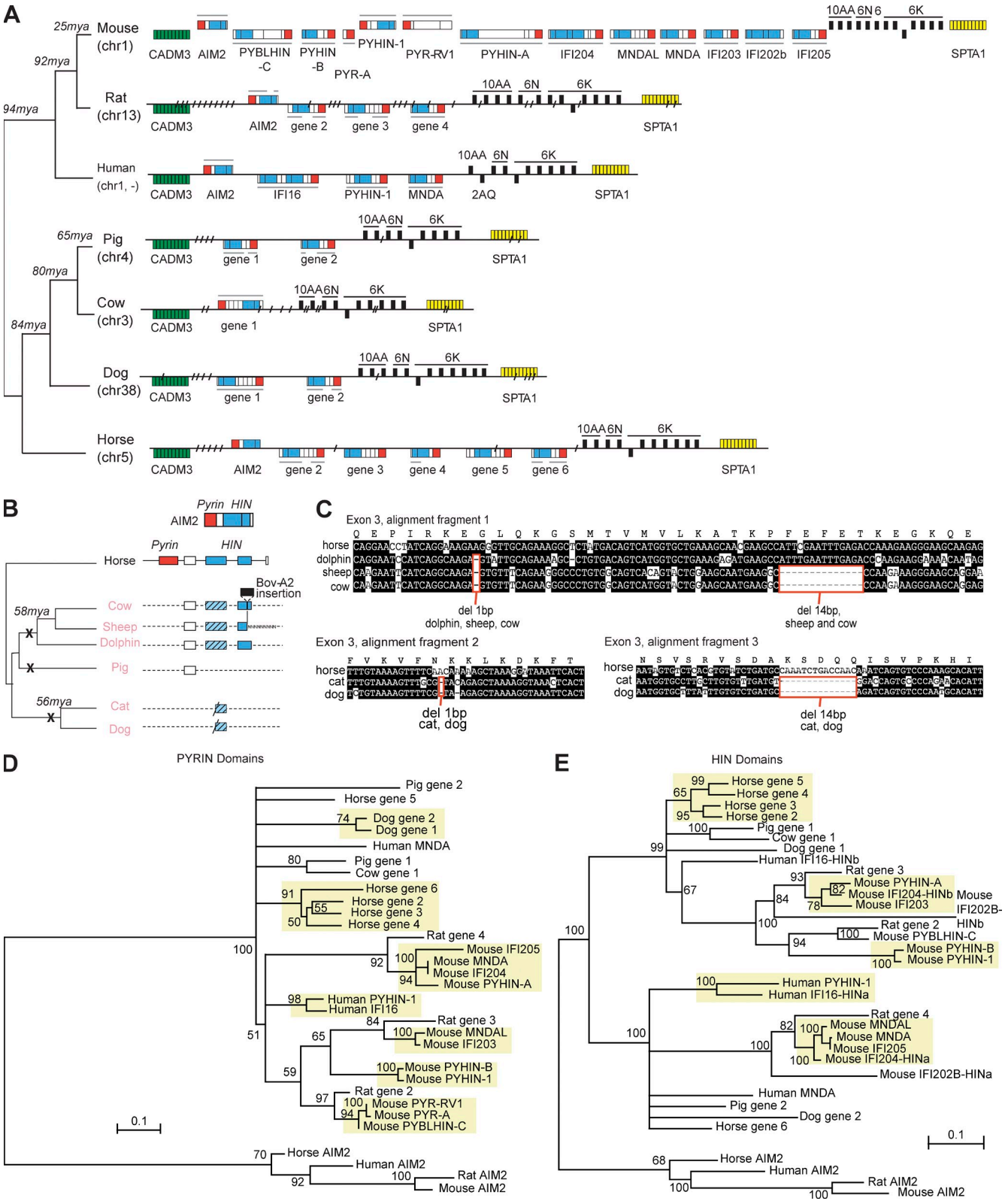

Figure 2. Evolutionary relationships of the ALR gene family in mammals. (A) Genomic loci containing ALRs in selected mammalian species (loci not drawn to scale). Boxes represent coding exons, with those encoding Pyrin domains in red and HIN domains in blue. Introns are omitted for clarity. ALRs from species other than mouse and human are arbitrarily named. Gray horizontal lines show which exon–exon boundaries are supported by mRNA or EST evidence; other boundaries are predicted computationally. Short diagonal lines indicate gaps in the genome assemblies. Flanking genes CADM3

the dog and cat genomes reveal that these two mammalian orders lost their *Aim2* gene at least 55 million years ago, although it was present in the last common ancestor of eutherian mammals (Fig. 2 C).

We used the sequences of these ALR open reading frames to construct separate phylogenetic trees for their Pyrin and HIN domains based on an alignment of their nucleotide sequences. These analyses reveal extensive evolutionary diversity within this gene family across species, as well as several specific features that have important implications for the biology of ALRs. First, the phylogenetic trees confirm that mouse, rat, human, and horse each have an orthologous *Aim2* gene based on gene location, orientation, and homology throughout both Pyrin and HIN domains, and validate *Aim2*'s absence from dog, pig, and cow (Fig. 2, D and E). Second, with the exception of the four-member *Aim2* "clade," the Pyrin and HIN trees reveal an almost complete lack of orthology among full-length ALR genes in any pairwise comparison between any mammalian species (Fig. 2, D and E) including the closely related species rat and mouse. For example, human *IFI16* and mouse *Ifi204* are considered orthologues because they both contain a single Pyrin domain and two HIN domains (Unterholzner et al., 2010). However, the phylogeny reveals that these two genes are not orthologous (each protein domain from IFI16 and IFI204 is more closely related to other genes). In fact, among the mammalian species we analyzed, there are no other Pyrin-containing ALRs that have two HIN domains, revealing that this domain organization is fortuitous rather than evolutionarily preserved from a common ancestor. Indeed, with the exception of AIM2 and "ALR gene 1" in pig and cow, no ALR is more closely related across its full length to an ALR in another species than it is to an ALR within the same species. The reason for this lack of orthology can be inferred from the numerous species-specific expansions (highlighted in yellow in Fig. 2, D and E) where protein domains of an ALR are much more closely related to ALRs from the same species, rather than to orthologues from other species. Whether because of independent gene duplications or recurrent gene conversions across the ALR genes, these patterns point to highly rampant species-specific specialization of ALRs.

Third, even within the same gene, the phylogeny of the Pyrin and HIN domains is often not congruent. Although in some instances, like in ALR gene 1 of pigs and cows, there is clearly a common history for both Pyrin and HIN domains, in most other instances, the Pyrin and HIN domains fall in completely disparate parts of the phylogeny (Fig. 2, D and E). This strongly suggests that recombination may have led not only to species-specific expansions of ALR genes, but also scrambled the existing genes into novel combinations of Pyrin and HIN domains.

This evolutionary analysis reveals a remarkable plasticity in mammalian ALR genes, with no single ALR gene preserved among all mammals and little orthology preserved across species. Instead, the ALR genes have undergone extensive, species-specific diversification, suggesting the existence of strong evolutionary pressures that have shaped ALR sequences and functions throughout the mammalian lineage. These data highlight the difficulty in applying conventional, sequence-based inference of ALR functions across even closely related mammalian species. For instance, the dramatic difference in the number and sequences of mouse and rat ALRs is caused by two factors: gene expansions in mouse of three ancestral rodent ALRs, and independent reassortment of the Pyrin and HIN domains that create additional diversity. Importantly, the three human ALRs (aside from AIM2) are not represented within these three rodent-specific clusters (Fig. 2, D and E). This completely revised view of ALR evolution challenges some of the interpretations of previous cross-species comparisons that have been made with the assumption of orthology, and necessitates the application of unbiased assays to test the function of each ALR within defined experimental conditions.

Most murine ALRs are abundantly expressed, and all are inducible

We focused on the murine ALR gene family for a more comprehensive analysis, with the hypothesis that characterizing all of these genes might reveal functional correlations to place within the evolutionary perspective characterized in Fig. 2. We developed and validated quantitative RT-PCR primers that specifically and efficiently amplify each of the 13 murine ALR open reading frames (Table S1 and not depicted). We determined the mRNA expression levels of each ALR in unstimulated bone marrow-derived macrophages and MEFs (Fig. 3 A and not depicted). We found

(green) and SPTA1 (yellow) have numerous exons that are not all presented here. Olfactory receptor genes and pseudogenes (black boxes) are also found at one end of the locus and are labeled according to their family and subfamily (e.g., 10AA = family 10, subfamily AA) using the HORDE system. A species tree (not to scale) is shown on the left, along with the approximate divergence times. The position of horse on the tree is uncertain (Meredith et al., 2011); we have depicted it in the position that is best supported by current evidence. Chromosomal locations of the locus are in parentheses, with a "−" symbol denoting that the human locus is depicted as flipped with respect to its numbered chromosomal orientation. (B) Using the horse AIM2 as a query in blast searches, we detected fragments of AIM2 pseudogenes in the genomes of cow, sheep, and dolphin, whereas pig *Aim2* appears to have only retained a recognizable exon 2. Cat and dog genomes only have a partial exon 3. (C) Three selected portions of a multi-species AIM2 alignment showing inactivating mutations shared by more than one species (red boxes). Highlighted bases are conserved in >50% of the sequences shown. These shared mutations show that the AIM2 gene was inactivated in the carnivore lineage before cat and dog diverged (~56 mya) and in at least some species of the Cetartiodactyla lineage since before dolphins, sheep, and cattle diverged (~58 mya). (D and E) Phylogenetic trees of the indicated mammalian ALRs based on Pyrin domains (D) and HIN domains (E). Species-specific ALR gene expansions are indicated in yellow boxes. Bootstrap values, calculated as described in the Materials and methods, are indicated at each branch point.

that 11 of the 13 ALRs are abundantly expressed, the 5 most abundant being PYHIN-A, MNDAL, PYHIN-1, IFI203, and PYBLHIN-C (Fig. 3 A). In contrast, we detected very little PYHIN-B or IFI202b mRNA in resting cells (Fig. 3 A). We determined the contribution of tonic type I IFN receptor signaling to the basal expression levels of each ALR mRNA by comparing WT and *Ifnar1*$^{-/-}$ macrophages. Interestingly, PYHIN-A and AIM2 expression was largely unaffected in *Ifnar1*$^{-/-}$ macrophages, whereas the basal expression of all other ALRs was reduced by at least 90% in the absence of IFN signaling (Fig. 3 A). We next quantitated the inducibility of each murine ALR in response to type I IFN treatment, activation of the ISD pathway, or activation of RIG-I. Consistent with findings reported for the 8 previously described ALRs, we found that all 13 murine ALRs are IFN-inducible genes, as indicated by increased expression levels 6 h after treatment with recombinant IFN-β in WT macrophages but not *Ifnar1*$^{-/-}$ macrophages (Fig. 3 B). The level of IFN-inducibility was inversely correlated with basal expression level: the most abundant ALRs were the least inducible, and the least abundant ALRs were the most inducible (Fig. 3 B). Interestingly, we found that ALR expression is dramatically increased after stimulation with ISD or RIG-I ligands, even in the absence of IFN signaling (Fig. 3 C). Together, these data provide a direct comparison of expression of all 13 murine ALRs and reveal 2 modes of ALR inducibility, one activated by IFNs and one activated by nucleic acid ligands.

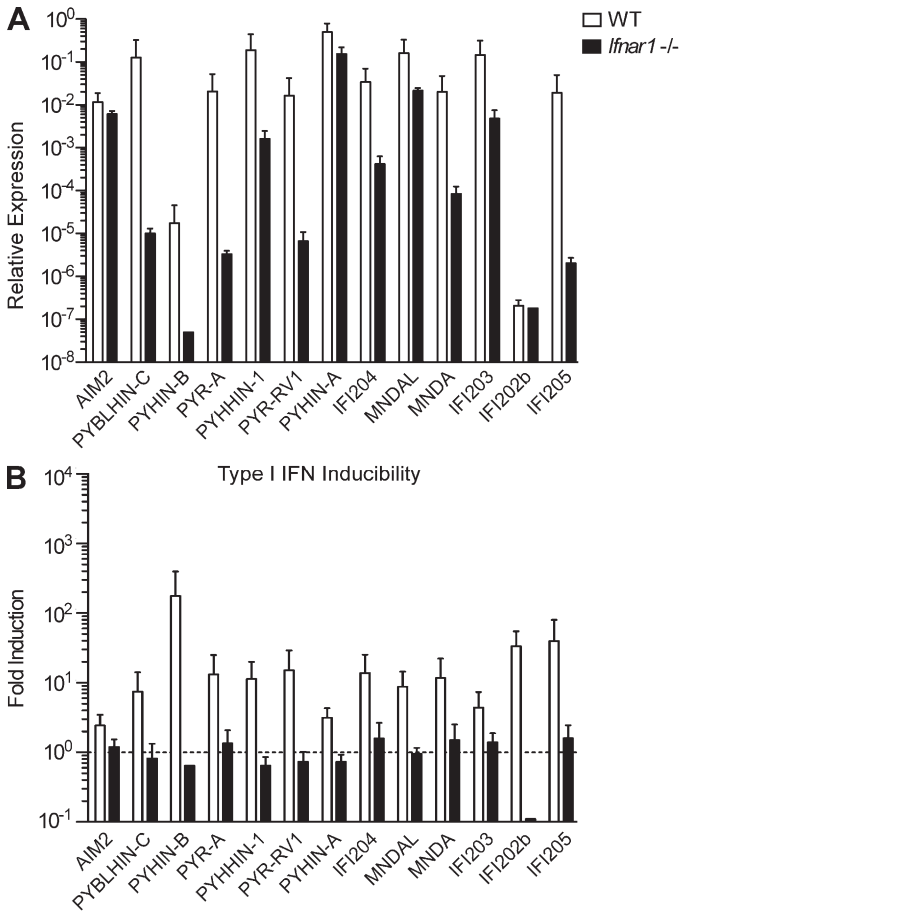

Figure 3. Expression and inducibility of murine ALR mRNAs. (A) Basal expression of each ALR mRNA in untreated WT and *Ifnar1*$^{-/-}$ BMDM, calculated relative to *HPRT* expression. (B) IFN-inducibility of murine ALRs: the basal expression level of each ALR was set to "1," and the fold induction of each ALR mRNA over untreated in WT and *Ifnar1*$^{-/-}$ BMDM is shown in response to a 6-h stimulation with 100 U/ml recombinant mouse IFN-β. (C) Ligand inducibility: CT DNA (1) or RIG-I Ligand (2). Results are representative of three experiments, with triplicate treatments in each experiment (error bars represent the SD [A] and the SEM [B and C]).

IFI204 is not a nonredundant sensor of DNA

Murine IFI204 was previously implicated as an antiviral sensor of DNA, based on proposed homology to human IFI16 and a ∼60% decrease in DNA-activated type I IFN production by murine cells in which IFI204 was knocked down (Unterholzner et al., 2010). However, our identification of novel ALRs, several of which are abundantly expressed and highly homologous to IFI204 in their Pyrin or HIN domains, along with the lack of true orthology between IFI16 and IFI204, raised the possibility that IFI204 itself

might not be a unique DNA sensor. We therefore designed lentiviral siRNAs targeting IFI204, taking into account the high sequence homology between IFI204 and other ALRs. We identified two different siRNAs that robustly reduced expression of an epitope-tagged IFI204 protein (Fig. 4 A), and verified knockdown of the corresponding endogenous IFI204 mRNAs in primary BM-derived macrophages (BMDMs) and MEFs (Fig. 4 B). One of these siRNAs also targeted MNDA, whereas the other was unique for IFI204 and no other murine ALR (Fig. 4, A and B, and not depicted). We transduced primary BMDMs and MEFs with these lentiviral IFI204 siRNAs or a control lentiviral siRNA-targeting GFP, selected the transduced cells to >99% purity in puromycin, and stimulated them with the entire panel of ISD and non-ISD ligands defined in Fig. 1. 4 h after treatment, we measured IFN-β induction by quantitative RT-PCR. We found that IFI204 knockdown did not reproducibly or specifically impair the ISD pathway in either BMDMs or MEFs (Fig. 4 C). We obtained identical results with stable IFI204 knockdown in *Ifnar1*$^{-/-}$ BMDMs, which respond robustly to ISD despite reduced basal expression levels of most ALRs (unpublished data). These data suggest that although IFI204 may contribute to the antiviral response, it is not uniquely required in either BMDMs or MEFs for full activation of the ISD pathway.

Murine ALRs have discrete patterns of localization in the presence of STING and ASC

The sequence homology among the Pyrin and HIN domains within the murine ALR family and the evolutionary diversity of ALRs among mammalian species led us to develop unbiased assays to quantitatively compare the localization and function of each ALR. We generated expression vectors encoding hemagglutinin (HA) epitope-tagged versions of all 13 murine ALRs and examined their localization after transfection into HeLa cells, which do not have a functional ISD pathway. We found that with the exception of AIM2, which is a cytosolic protein (Hornung et al., 2009), the other 12 murine ALRs localized exclusively to the nucleus when expressed alone (Fig. 5 A, left two columns). We next determined the localization of each ALR upon coexpression with either STING or ASC, which are required for DNA-activated IFN production and inflammasome triggering, respectively. Interestingly, most of the 13 ALRs colocalized with STING, either partially or entirely, when overexpressed with STING alone unpublished data). Similarly, all 13 ALRs colocalized with ASC when overexpressed with ASC alone, and again, the extent of colocalization varied from partial to complete (unpublished data). Thus, all ALRs relocalize when expressed with relevant adaptor proteins, and coexpression of an ALR with a single adaptor protein reveals indiscriminate colocalization. We therefore expressed each ALR together with both STING and ASC to more closely approximate the expression of all three proteins in macrophages and other cell types. These experiments revealed three predominant localization patterns of murine ALRs that were not apparent when each ALR was expressed alone or with a single adaptor protein. The first pattern, exemplified most clearly by AIM2, MNDA, and MNDAL, was a strong colocalization with puncta of ASC and minimal colocalization with STING (Fig. 5 A). The second pattern, most evident with PYHIN-B, PYR-A, PYHIN-1, PYHIN-A,

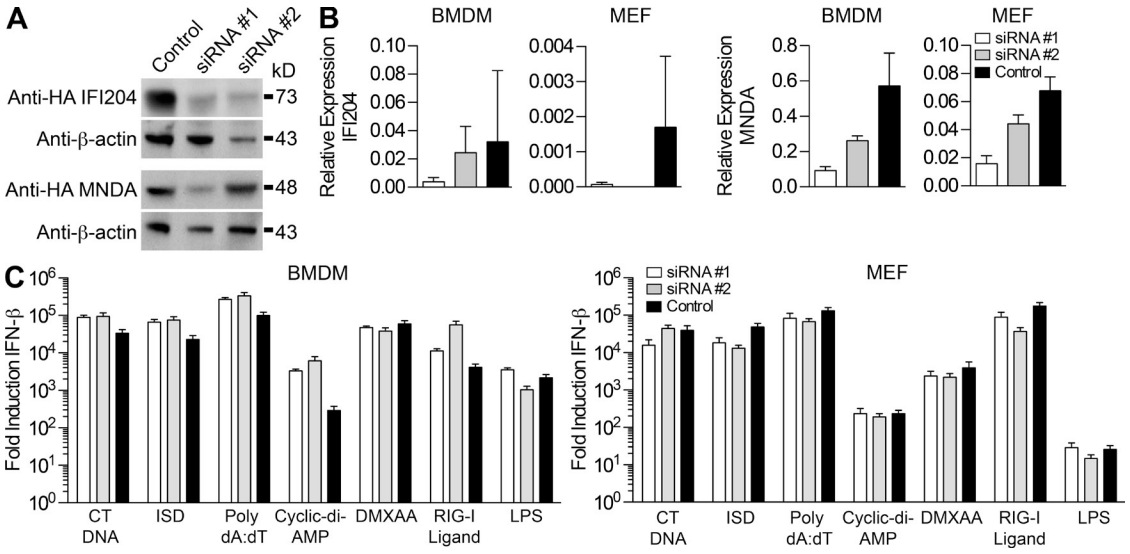

Figure 4. Murine IFI204 is not a nonredundant sensor of DNA. (A) Knockdown efficiency in HEK293T cells transiently transfected with 500 ng HA-tagged IFI204 and 2 µg siRNA #1, siRNA #2, or control siRNA for 24 h. IFI204 protein knockdown was assessed by anti-HA immunoblot (IB). (B) Quantitative real-time PCR of IFI204 mRNA expression in BMDM (left) and MEF (right) stably expressing the indicated lentiviral siRNA constructs. (C) Quantitative RT-PCR analysis of IFN-β mRNA expression in BMDM and MEF stably expressing the indicated lentiviral siRNAs and treated as indicated for 4 h before harvest. Results are representative of two independent experiments, each with triplicate treatments for each ligand (error bars represent the SD [B] and the SEM [C]). Statistical analysis was performed with a two-way ANOVA test, and none of the stimulated knockdown cells reached a statistical significance of $P < 0.05$ compared with control cells.

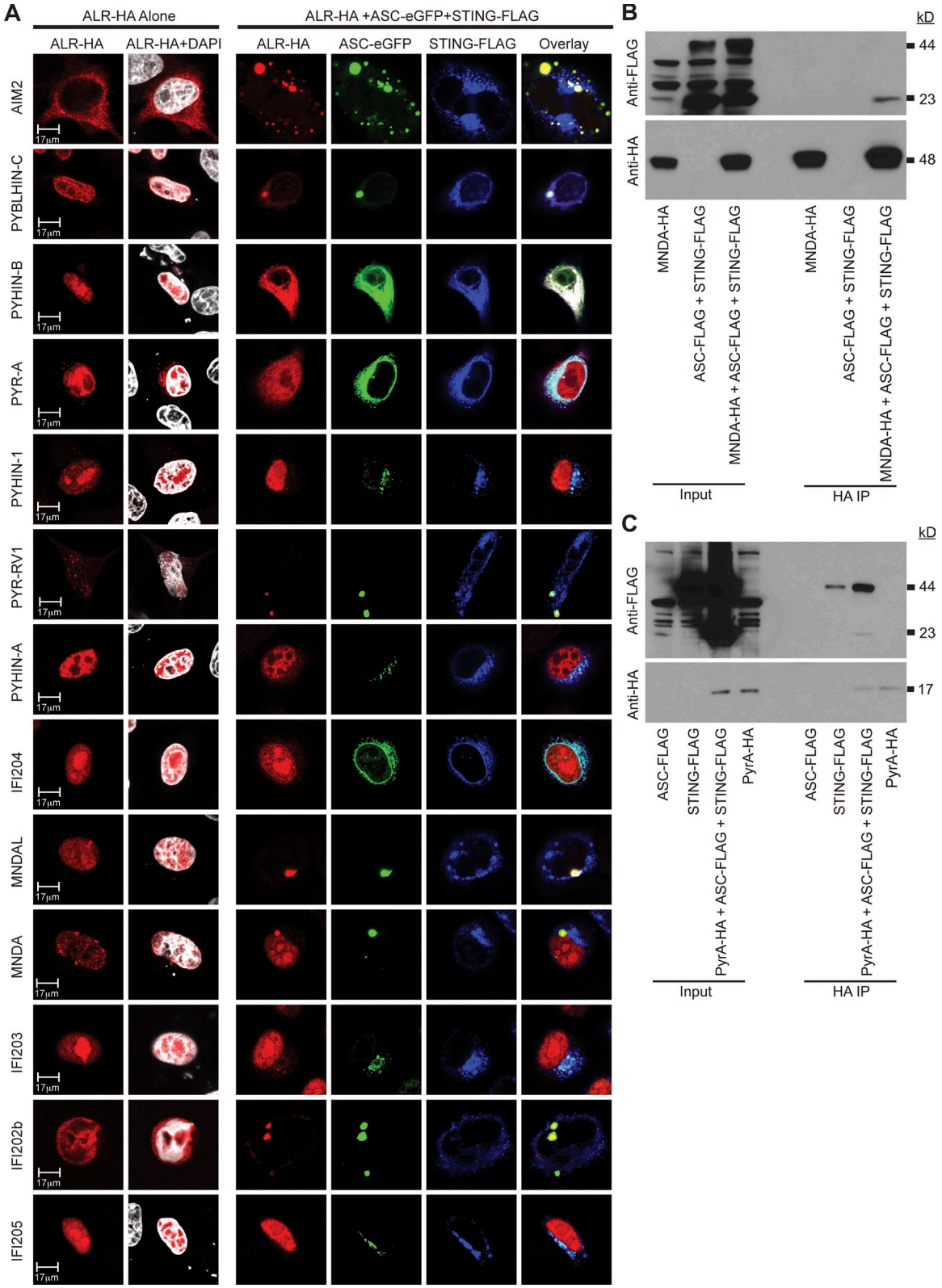

Figure 5. Intracellular localization of murine ALR proteins. (A) 500 ng ALR-HA expression plasmids alone (left two columns) or 500 ng ALR-HA, 500 ng ASC-eGFP, and 500 ng STING-FLAG (right columns) were transfected into 3.0×10^4 HeLa cells and probed 24 h after transfection with anti-HA-ALR (red), anti-eGFP (green), anti-FLAG (blue), and DAPI (gray). (B) HA-tagged murine MNDA was immunoprecipitated from control cells and cells expressing STING-FLAG and ASC-FLAG, which can be distinguished based on their size despite the same tag. (C) HA-tagged Pyr-A was immunoprecipitated from cells expressing the indicated constructs, followed by blotting for STING-FLAG and ASC-FLAG. All data are representative of three to five independent experiments.

IFI204, IFI203, and IFI205, was a predominant colocalization with STING in structures that resemble previously defined STING-positive ER–Golgi compartments (Ishikawa and Barber, 2008), together with a concomitant recruitment of ASC to these areas of ALR-STING colocalization. The remaining three ALRs (PYBLHIN-C, PYR-RV1, and IFI202B) localized to ASC puncta with detectable, but not complete colocalization of STING. We confirmed the specificity of these interactions for two of the novel ALRs by coimmunoprecipitation in cells expressing STING and ASC. In agreement with the microscopy data, we found that MNDA interacted with ASC but not STING (Fig. 5 B), and that PyrA interacted with both STING and ASC, with the ASC interaction significantly weaker than the STING interaction (Fig. 5 C). Together, these data reveal that murine ALRs can be categorized based on their ability to be recruited to ASC, STING, or both.

Novel murine and human ALR activators of STING-IFNs and the ASC-inflammasome

We developed simple assays to evaluate and compare the functional capabilities of all murine and human ALRs. We found that overexpression of each murine and human ALR alone did not activate an IFN-stimulated response element (ISRE) luciferase reporter in HEK293T cells (unpublished data). We therefore included coexpression of STING at a concentration that was insufficient to activate the ISRE-luciferase reporter on its own (Fig. 6 A). Interestingly, we found that several murine ALRs robustly activate STING-dependent IFN production. The strongest activator of STING was the Pyrin-only protein PYR-A, and among the full-length ALRs we observed the strongest IFN induction by PYHIN-A and IFI203 (Fig. 6 A). IFI202b, which has two HINs but no Pyrin domain, also activated a robust STING-dependent IFN response, suggesting that a Pyrin domain is not required for this activity in cis. The remaining ALRs exhibited weak or minimal STING-dependent activity, as exemplified by AIM2, consistent with the intact ISD pathway in AIM2-deficient murine cells (Hornung et al., 2009).

We next generated HEK293T cells that stably express ASC and caspase-1 for evaluation of inflammasome activation by murine ALRs. We co-transfected plasmids encoding each ALR with an expression vector for full-length murine

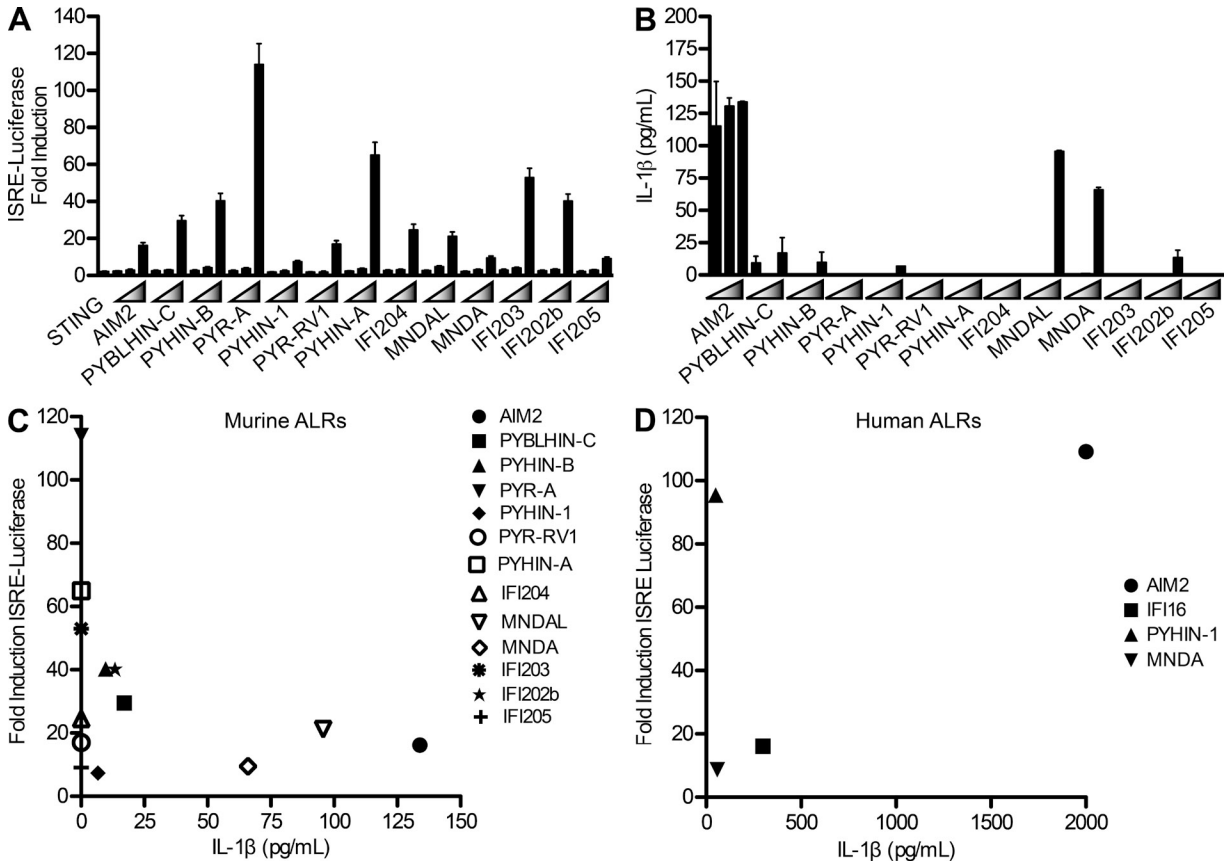

Figure 6. Unbiased functional characterization of all mouse and human ALRs. (A) ISRE luciferase reporter assay in HEK293T cells transiently transfected with ISRE luciferase reporter and increasing amounts of ALR-HA expression vectors with 300 ng STING-FLAG vector, measured 24 h after transfection. Results are expressed as fold induction over ISRE-luciferase alone. (B) IL-1β ELISA of HEK293T cells stably expressing murine ASC-FLAG and murine caspase-1, transfected with increasing amounts of ALR-HA expression vectors and 100 ng pro-IL-1β vector. (C) Plot of ISRE luciferase induction versus IL-1β secretion for each ALR. (D) Plot of ISRE-luciferase induction versus IL-1β secretion for each human ALR. Results are representative of 2–5 experiments, with each treatment done in triplicate (error bars represent the SEM [A] and the SD [B]).

IL-1β and measured inflammasome activation using an ELISA for secreted IL-1β. ALR-activated IL-1β secretion was undetectable in the parental HEK293T cells or in cells stably expressing ASC alone or caspase-1 alone, validating the specificity of this assay (unpublished data). As expected, we found that overexpression of murine AIM2 potently activated IL-1β secretion (Fig. 6 B). Interestingly, we identified two additional murine ALRs (MNDA and MNDAL) as novel and robust activators of the ASC inflammasome (Fig. 6 B). The remaining 10 murine ALRs exhibited minimal or undetectable IL-1β processing activity in this assay. Thus, three murine ALRs are capable of activating the inflammasome.

We plotted the ability of each murine ALR to activate STING-dependent IFN production versus ASC-dependent IL-1β processing, thus creating an activity map of the entire murine ALR family. We found largely nonoverlapping activities of each murine ALR in these assays, such that individual ALRs robustly activate either STING-IFN (PYR-A, PYHIN-A, IFI203, PYHIN-B, and IFI202b), ASC-inflammasome (AIM2, MNDA, and MNDAL), or neither (Fig. 6 C). Importantly, the ability of an individual ALR to activate STING or ASC closely correlated with its colocalization with these adaptors (Fig. 5), validating the predictive value of these cell biological and functional assays.

We next performed the same ISRE and IL-1β assays with the four human ALRs and uncovered novel activities. Interestingly, whereas murine AIM2 activates ASC but not STING, human AIM2 robustly activates both pathways, making it the only ALR among the 17 tested that has dual activity (Fig. 6 D). Moreover, we found that human PYHIN-1 is a novel, robust, and specific activator of STING-dependent IFN production (Fig. 6 D). In contrast, human IFI16 and MNDA did not strongly activate either STING or ASC in these assays, although IFI16 showed detectable activation of STING-IFN and ASC-inflammasome, consistent with previous studies (Unterholzner et al., 2010; Kerur et al., 2011). These data provide an unbiased functional characterization of all currently known murine and human ALRs, revealing several novel activators of STING and ASC.

DISCUSSION

The innate immune response triggered by detection of intracellular DNA is important for host defense and causes several specific human autoimmune diseases, but the receptors that activate this response have remained elusive. In this study, we present a phylogenetic analysis of the ALR gene family, together with an extensive characterization of the expression, localization, and function of all known mouse and human ALRs. Our results validate the principal findings of the first studies that identified specific ALRs as important components of the DNA-activated inflammasome (Bürckstümmer et al., 2009; Fernandes-Alnemri et al., 2009; Hornung et al., 2009; Roberts et al., 2009) and the STING-dependent ISD pathway (Unterholzner et al., 2010), and we identify several novel activators of these two pathways among human and mouse ALRs. Together, these data provide an evolutionary foundation and a functional framework for understanding the role of ALRs in host defense.

Our phylogenetic analysis of ALRs reveals several interesting features of this gene family, with important evolutionary and biological implications. On a practical level, the lack of preserved orthology between human and mouse ALRs (AIM2 excepted) means that a new nomenclature will need to be established for these genes, especially for those ALRs (MNDA and PYHIN-1) that have the same name in mouse and human but are neither evolutionary nor functional orthologues (Figs. 2 and 6). Interestingly, our functional analysis reveals that the two previously defined functions of STING-IFNs and ASC-inflammasome are preserved among the repertoire of murine and human ALRs, despite this lack of sequence orthology at the level of individual genes. Moreover, we found that there are multiple ALRs capable of activating STING-IFNs and multiple ALRs capable of activating the ASC-inflammasome (Fig. 6). We propose that this functional redundancy, together with the remarkable diversity of ALRs among even closely related species, reflects strong evolutionary pressures placed on the ALR gene family by pathogens (likely DNA viruses). Importantly, these selective pressures are pervasive throughout the mammalian lineage, and no single ALR is conserved as a functional gene in all mammals. The expansion of the murine ALR locus is the most dramatic among the mammals we examined, and our preliminary analysis of this locus in other strains of mice suggests that the numbers of ALR genes and pseudogenes differ among strains (unpublished data). Such strain-specific differences in ALR gene composition might explain the contribution of ALRs to lupus susceptibility in certain inbred mice (Rozzo et al., 2001). This species-specific diversification is unusual among candidate innate immune response genes, but not unprecedented. For example, the genes encoding the NOD-like receptors with pyrin domains (NLRPs; Elinav et al., 2011), the APOBEC3 family of cytidine deaminases (Harris and Liddament, 2004), and the immunity-related GTPases (IRGs; Kim et al., 2011) are all dramatically different in composition and number between humans and rodents.

We characterized the localization of all murine ALRs, in the absence and presence of STING and ASC, revealing that 12 of the 13 ALRs are nuclear proteins but move to localize with the adaptor proteins upon overexpression-induced signaling (Fig. 5). The first studies that identified the DNA-activated antiviral response suggested that detection of DNA likely occurs in the cytosol, thus offering a simple compartment-based explanation for how these pathways distinguish foreign from self DNA. However, it is important to note that nearly all DNA viruses, including those that have been implicated as ALR activators (Unterholzner et al., 2010; Kerur et al., 2011), replicate in the nucleus. Thus, the steady-state nuclear localization of nearly all murine and human ALRs may position these receptors to respond to specific replication

intermediates of DNA viruses and retroelements (Fig. 5; Hornung et al., 2009). How these receptors distinguish microbial DNA from host genomic DNA, and how they move to the cytosol to form signaling complexes with STING and/or ASC are important questions for future study. We observed this movement from the nucleus to form signaling complexes with STING or ASC for nearly all murine ALRs, and the localization patterns correlated strongly with the functional assays (Fig. 5 and Fig. 6). We found that the STING-activating ALRs recruited ASC to STING, but the ASC activators did not recruit STING to ASC (Fig. 5). This finding hints at a potential explanation for why ASC-deficient cells have a hyperresponsive ISD pathway (Hornung et al., 2009), yet STING-deficient cells have a normal DNA-activated inflammasome response (not depicted). We suggest that this inducible recruitment of ASC to STING during ISD pathway activation is a negative regulatory event, the cell biology of which will be an interesting area for future research.

Our phylogenetic analysis of ALR diversity and the lack of known functions for most ALRs prompted us to develop simple, unbiased assays to determine the functional capabilities of each ALR and compare these functions among all of the ALRs in mice and humans. Using these assays, we uncovered novel ALRs that activate STING-dependent IFNs and the ASC inflammasome. Among the murine ALRs that potently activate STING, we found one Pyrin-only protein (PYR-A), one HIN-only protein (IFI202b), and two additional full-length ALRs (PYHIN-A and IFI203). These data reveal considerable functional redundancy among the ALR gene family in mice and suggest that both Pyrin and HIN domains can independently contribute to STING activation. Interestingly, for the three full-length murine ALRs that strongly activate STING defined here and elsewhere (PYHIN-A, IFI203, and IFI204; Unterholzner et al., 2010), their HIN domains cluster together on the phylogenetic tree but their Pyrin domains do not (Fig. 2 C). We found two novel activators of the ASC inflammasome among murine ALRs (MNDA and MNDAL). However, AIM2-deficient mouse cells are profoundly impaired for the DNA-activated inflammasome (Rathinam et al., 2010), so neither MNDA nor MNDAL are functionally redundant with AIM2, at least for the ligands and microbes used in these studies. We suggest that the nuclear MNDA and MNDAL receptors might respond to unique ligands or to a specific class of viruses that is not sensed by AIM2. Additionally, we revealed novel functions for human ALRs. Of the 17 murine and human ALRs examined, human AIM2 is the only ALR capable of activating both IFNs and the inflammasome (Fig. 6). In contrast, the AIM2 orthologue in mouse (a rare example of clear sequence orthology in this family) activates the inflammasome, but not IFNs. We propose that other, currently uncharacterized ALRs might have dual functionality, and that the loss of AIM2 in numerous mammalian species (Fig. 2) might be compensated for by other ALRs that activate the inflammasome, thus preserving this important innate immune function. Interestingly, we found that human PYHIN-1, an ALR with no previously described function, potently activates STING-dependent IFN production (Fig. 6). This potential antiviral function of PYHIN-1 provides a mechanistic basis for further study of the recently identified human *PYHIN1* polymorphisms associated with asthma in African Americans (Torgerson et al., 2011). Finally, we found several ALRs that had little detectable activation of either STING-IFNs or ASC-inflammasome. These ALRs may activate a response distinct from the ones we measured, they could require additional cofactors for activation, or they could be negative regulators of the other ALRs. Because several ALRs are coexpressed in cells (Fig. 3), the net outcome of activating multiple ALRs at once may be different from the activation of individual ALRs in isolation. Overall, although we cannot infer in vivo function or ligand specificity from these studies, we emphasize that the utility of these assays lies in the direct, unbiased comparison of all ALRs, thus creating a map of ALR function that will guide future efforts to understand these receptors.

We found, using stable lentiviral knockdowns in primary macrophages and MEFs, that murine IFI204 is not a unique activator of the ISD pathway (Fig. 4). Moreover, we found that lentiviral knockdown of each of the murine ALRs individually had no significant effect on ISD sensing (unpublished data). Although others have shown a contribution of murine IFI204 to the DNA-activated IFN response (Unterholzner et al., 2010), knockdown of IFI204 in these studies did not completely abolish ISD sensing, suggesting that other receptors might contribute to this pathway. In light of our identification of several novel ALRs in mice that are closely related to IFI204, and our data revealing additional ALRs that activate STING, we suggest that multiple ALRs might be responsive to ISD ligands, similar to the way that transfected poly(I:C) can activate both RIG-I and MDA5 (Kato et al., 2008). Based on these findings, complete characterization of the ALR gene family will require the generation of mouse models deficient in all ALRs.

In closing, our findings reveal the evolutionary diversity and functions of mammalian ALRs, and offer several possible explanations for why the dissection of ISD sensors has remained elusive despite several years of intense efforts. First, the use of "pure" ISD ligands that uniquely trigger the STING-dependent antiviral response is important because certain DNA polymers trigger two largely redundant pathways (Fig. 1). Second, the ALR gene family has little preserved orthology among mammals, complicating efforts to understand ALR function without the clear phylogenetic picture of ALR evolution that we provide here (Fig. 2). Third, individual ALRs are functionally inert when overexpressed on their own in the cell lines used for these assays (Fig. 6), thus rendering these receptors "invisible" to the conventional expression cloning approaches used to identify RIG-I/MDA5 (Yoneyama et al., 2004), MAVS (Kawai et al., 2005; Seth et al., 2005), and STING (Ishikawa and Barber, 2008). Finally, we show that multiple mouse and human ALRs are competent for STING activation (Fig. 6),

suggesting a functional redundancy among these ALRs that may complicate genetic approaches and RNAi-based screens to identify ISD sensors. Together, the data presented here create a framework for investigating the role of ALRs in the antiviral response.

MATERIALS AND METHODS

Mice and cells. C57BL/6 mice were purchased from The Jackson Laboratory. *Tmem173*$^{-/-}$ mice (provided by G. Barber, University of Miami, Miami, FL) were generated as previously described (Ishikawa and Barber, 2008), backcrossed to C57BL/6 mice, and screened by genome-wide single-nucleotide polymorphism analysis until they were >99.8% C57BL/6. *Mavs*$^{-/-}$ mice (provided by M. Gale, Jr., University of Washington, Seattle, WA) were generated on a C57BL/6 background as previously described (Gall et al., 2012), and *Ifnar1*$^{-/-}$ mice that had been backcrossed >10 times to C57BL/6 were provided by M.-K. Kaja (Emory University, Atlanta, GA). BMDMs, BMDCs, and primary, early passage MEFs were generated and cultured according to standard techniques. WT controls for all experiments were age-matched C57BL/6 mice. All animals were maintained in accordance with guidelines of the University of Washington Institutional Animal Care and Use Committee. HEK293T were purchased from Invitrogen and HeLa cells were purchased from American Type Culture Collection. HEK293T reporter cells stably expressing ASC, caspase 1, or ASC/caspase1 were generated by stable transfection and tested for expression of the relevant proteins.

Cell treatments and analysis. ISD oligonucleotides were annealed (Stetson and Medzhitov, 2006), and RIG-I ligand was in vitro transcribed as previously described (Saito et al., 2008). BMDMs and BMDCs were plated at a density of 0.7×10^6, and MEFs were plated at 0.2×10^6 per well, in 12-well plates for transfection. For transfections, 5 µg calf thymus genomic DNA (Sigma-Aldrich), 5 µg ISD, 5 µg poly dA:dT (Invitrogen), 2.5 µg cyclic-di-AMP (BioLog), and 1 µg RIG-I ligand were complexed with Lipofectamine 2000 (Invitrogen) at a ratio of 1 µg nucleic acid to 1 µl lipid. 30 µg/ml DMXAA (Sigma-Aldrich) and 10 ng/ml LPS (Sigma-Aldrich) were added directly to the culture media. For quantitative RT-PCR of IFN-β or ALR mRNA, cells were harvested into RNA-Bee (Teltest). RNA was reverse transcribed with Superscript III (Invitrogen), and cDNAs were used for PCR with EVA Green reagents (Bio-Rad Laboratories) on a Bio-Rad CFX96 Real-Time System. The abundance of each cytokine mRNA was normalized to HPRT expression and compared with untreated cells to calculate the relative induction. Primers for IFN-β and HPRT were described previously (Stetson and Medzhitov, 2006), and primers for quantitative RT-PCR analysis of murine ALR expression are listed in Table S1.

Bioinformatic analysis of mammalian ALRs. We used queries to the genes that flank the ALR locus in mammals, *CADM3* (cell adhesion molecule 3) and *SPTA1* (spectrin, α, erythrocytic 1) to identify the syntenic region in other mammalian genomes via the University of California Santa Cruz Genome Browser (Kent et al., 2002). The species and genome sequence versions we used are as follows: *Mus musculus* (mouse), mm9, July 2007; *Rattus norvegicus* (rat), rn4, Nov. 2004; *Homo sapiens* (human), hg19, Feb. 2009; *Equus caballus* (horse), equCab2, Sept. 2007; *Canis familiaris* (dog), canFam2, May 2005; *Bos taurus* (cow), bosTau6, Nov. 2009; *Sus scrofa* (pig), susScro2, Nov. 2009. We refined the annotation and description of the olfactory receptor genes using minor modifications to a previously described bioinformatics pipeline (Young et al., 2002).

To annotate ALRs in the genomes of species other than human and mouse we considered multiple lines of evidence. We first used amino acid sequences of the human and mouse ALRs we identified as queries in tblastn searches of each genome assembly. We parsed the tblastn output using a custom Bioperl script (Stajich et al., 2002), and displayed the locations of matching sequence regions as a custom track on the University of California Santa Cruz browser, keeping even weak matches to ALRs. In some cases, scrutiny of the tblastn search results revealed that a stop codon or frameshift interrupted some ALR coding fragments; we annotated such ALRs as pseudogenes (data not shown). We also performed a similarity search using just the Pyrin and HIN domains alone, allowing us to more easily visualize domain organization. Pyrin domain matches were often found very close in the genome to matches to both exons of the HIN domain. Indeed, if we use the criteria of identifying all Pyrin domains found within 1 MB of HIN domains, we did not find any putative ALR genes outside the ALR locus. However, within the syntenic ALR loci, we also considered pyrin-domain or HIN-domain matches alone as candidate genes (see main text).

We next examined the coordinates of mapped expressed sequence tags (ESTs), experimentally determined mRNAs and known genes. We used those mapped sequences to define ALR intron–exon boundaries, considering any sequences that overlapped the aforementioned tblastn matches. We next compared the results of our curated analyses to the ab initio gene predictions from gene-finding algorithms like Genscan reported in the Ensembl database. We performed blastp (protein–protein) searches of the Ensembl dataset using the full-length human and mouse ALRs as queries.

We integrated information from the three sources described above (tblastn searches, EST analysis, and Ensembl predictions) to make a combined ALR gene prediction. EST or mRNA sequences provided the most high-confidence delineation of intron–exon boundaries: many ESTs were available for many ALRs, covering most or all of the gene. Most predicted ALRs were typical of the human and mouse ALRs we characterized in detail experimentally, containing 6–8 coding exons whose predicted protein sequence contains both a pyrin and a HIN domain. We compared our EST-based predictions with Ensembl predictions where they overlapped and found that some ALRs appear well-predicted by Ensembl's pipeline. However, some of Ensembl's predictions include a large number of tiny exons, which is likely a misprediction of exon/intron boundaries. We therefore only used Ensembl's gene predictions for regions of ALR genes where EST/mRNA information was partially or entirely missing. One caveat of our analyses is that although the mouse and human genome assemblies are of very high quality in the ALR locus, the other assemblies are still in draft form and contain some gaps in the region. We would expect most ALRs to be at least partially represented in the draft assemblies, but very recently duplicated genes are unlikely to be resolved and might be represented by just a single sequence.

Following up on our initial observations that full-length AIM2 was missing in some genomes, we performed additional analyses. To find direct evidence of an AIM2 pseudogene, we used the nucleotide sequence of the AIM2 orthologue from horse (the most closely related species that contains a functional AIM2) as query in a blastn search of the cow, dog, and pig genome assemblies described above, as well as in searches of lower coverage genome assemblies of dolphin (*Tursiops truncatus*, turTru1, 2.6× coverage), sheep (*Ovis aries*, oviAri1, Feb. 2010, ∼3× coverage), and cat (*Felis catus*, felCat4, Dec. 2008, ∼2.8× coverage). We examined all hits that clearly matched functional AIM2 sequences better than any other ALR, and thus comprise partial AIM2 orthologues. We found cow, sheep and dolphin sequences that match the second, third, and fourth coding exons of AIM2, dog and cat sequences that match the third coding exon of AIM2 (the first part of the HIN domain), and a pig sequence that matches the second coding exon of AIM2 (between the pyrin and HIN domains; Fig. 2 b and Fig. S2). We did not find full-length copies of AIM2 in any of these genomes. Blastx searches revealed that each species' AIM2-like sequences contained frameshifts and/or premature stop codons. These results together indicate AIM2 is a degenerate, unprocessed pseudogene in cow, dog, and pig (and related genomes). We used TimeTree (www.timetree.org) to estimate divergence times between mammalian species and to date the common events that led to pseudogenization of AIM2 in some species. Given that large portions of the AIM2 gene appear to have been deleted in each of these genomes, it is not possible to determine whether the two lineages lost AIM2 function independently, or whether their common ancestor had already experienced AIM2 inactivation.

Phylogenetic analysis of mammalian ALRs. We separately aligned sequences of each pyrin domain and each HIN domain (sequences outside those domains did not align well) and made phylogenetic trees. For this, we first produced amino acid alignments by obtaining seed alignments of HIN (PF02760) and Pyrin (PF02758) domains from PFAM (Punta et al., 2012). We edited PFAM's pyrin alignment to retain sequences from the ALR locus and only one outgroup sequence (NAL12). We used hmmbuild from the HMMER package (http://hmmer.janelia.org, version 3.0) to make a hidden Markov model (HMM) representing each alignment. We then used HMMER's hmmsearch algorithm to identify those domains in each of the predicted ALR protein sequences, specifying the -A option to automatically output domain sequences aligned to the HMM. This amino acid alignment was then used to generate a corresponding nucleotide alignment that retained codon information. This nucleotide alignment was used to generate a PhyML bootstrap tree (www.phylogeny.fr) using either a HKY85 or GTR (general time reversible) model of nucleotide substitutions (GTR results are reported in Fig. 2c). Bootstrap values were calculated as a percentage of 1,000 trials. Phylogenies were visualized and formatted using the Dendroscope software (Huson et al., 2007). All nodes with bootstrap values of <50% were collapsed for ease of presentation.

Lentiviral siRNA knockdowns. IFI204 and control siRNA constructs were designed and cloned into the pLKO.puro plasmid. IFI204 and MNDA are targeted by siRNA #1 sequence (sense): 5′-CCAAGAGCAATACACCACGAT-3′. siRNA #2 exclusively targets IFI204 sequence: 5′-GCTAAGGAAGAAGATCACCAT-3′. The control siRNA targets eGFP: 5′-CAACAAGATGAAGAGCACCAA-3′. Knockdowns were validated by transfecting 2×10^5 HEK293T cells in 12-well plates with 500 ng-1 µg HA-tagged IFI204 expression vector along with 1–2 µg of either control or IFI204-specific pLKO.1 vector. 24 h later, IF204 knockdown in whole-cell extracts was evaluated by Western blotting with anti–HA-Tag (6E2) mouse monoclonal antibody (Cell Signaling Technology) according to standard techniques.

For IFI204 knockdown in BMDMs and MEFs, VSV pseudotyped lentivirus for stable transduction was produced by transfecting 2.5×10^6 HEK293T cells in 10-cm plates with 10 µg of pLKO siRNA knockdown construct, 9 µg psPAX-2, and 1 µg pVSV-G for 48 h. 4×10^6 BMDMs and 2.5×10^6 MEF were transduced with HEK293T viral supernatants, selected with 5 µg/ml puromycin (Invitrogen) for 3 d, and plated for ligand treatments.

Immunofluorescence microscopy. ALR cDNAs were cloned into pCDNA.3 with a C-terminal HA-tag (Fig. S2). The open reading frame of murine STING was cloned into pCDNA.3 with a C-terminal FLAG-tag, and murine ASC was subcloned from pCDNA.3 into pEGFP-N1 to create a plasmid expressing an ASC-eGFP fusion protein. 3×10^4 HeLa cells plated on glass coverslips in 24-well plates were transfected with 500 ng HA-tagged ALR alone, or together with 500 ng STING-FLAG and/or 500 ng ASC-EGFP. 24 h later, cells were fixed with 2% paraformaldehyde in PBS for 15 m, permeabilized for 15 m with 0.1% Triton-X 100 PBS, and blocked in 2% FCS PBS for 1 h at room temperature. Cells were stained with anti–HA-Tag (6E2) mouse monoclonal antibody (Cell Signaling Technology; 1:200), and anti-DDDDK FLAG rabbit polyclonal antibody (Abcam; 1:200) for 1 h, washed, and stained with anti–mouse Alexa Fluor 568 (Invitrogen; 1:200), anti–rabbit Alexa Fluor 647 (Invitrogen; 1:200) and then directly conjugated rabbit anti-GFP Alexa Fluor 488 (Invitrogen; 1:200) for 1 h at room temperature. Coverslips were mounted with SlowFade Gold with DAPI (Invitrogen) and visualized by microscopy with a Nikon A1RSi Scanning Laser Microscope (Nikon). Images were acquired with a Plan Apo VC 60× Oil DIC N2 objective (Nikon) in the 405, 488, 561, and 638 dichroic channels with NIS-Elements Software (Nikon) and pseudocolored with Fiji open source software.

Luciferase and IL-1β reporter assays. 1.3×10^5 HEK293T cells in 24 well plates were transfected with 25 ng ISRE-luciferase reporter plasmid (Takara Bio Inc.) with 0, 100, or 300 ng or 1 µg of pCDNA.3-expressing HA-tagged ALRs, alone or together with 300 ng STING-FLAG expression vector, and then incubated for 24 h. Cells were lysed and luciferase activity was assessed using the Luciferase Reporter Assay System (Promega) according to the manufacturer's instructions and read using a Centro LB 960 Luminometer (Berthold Technologies). Inflammasome reporter cells were generated by single-cell cloning of HEK293T cells stably expressing murine ASC-FLAG and murine caspase-1. Cells were plated at a density of 1.3×10^5 in 24-well plates and transfected for 48 h with 0, 100, or 300 ng or 1 µg of HA-tagged ALR expression vectors with 100 ng of pCDNA3.1-pro-IL-1β expression vector. The supernatant was harvested and assayed for IL-1β secretion using a mouse IL-1β ELISA Set (Becton Dickinson) according to the manufacturer's instructions. ELISA plates were read using an iMark Microplate Reader (Bio-Rad Laboratories).

Online supplemental material. The supplemental text shows open reading frames of 13 ALRs in C57BL/6 mice. Table S1 shows primers for quantitative RT-PCR analysis of murine ALR expression. Online supplemental material is available at http://www.jem.org/cgi/content/full/jem.20121960/DC1.

We are grateful to Michael Gale, Jr., for providing *Mavs*$^{-/-}$ mice, to Glen Barber (University of Miami) for providing *Tmem173*$^{-/-}$ mice, to Murali-Krishna Kaja for the *Ifnar1*$^{-/-}$ mice, to Jeff Duggan for cloning the human ALRs, to Elizabeth Kopp (Yale University) for ASC-FLAG expression vector, and to members of the Stetson laboratory for helpful discussions.

Supported by the National Institute of Allergy and Infectious Disease (AI084914, 5U54AI057141-08; D.B. Stetson), the European Union (FP7/2007-2013) grant agreement number 241779 to D.B. Stetson, the Lupus Research Institute (D.B. Stetson), and the Howard Hughes Medical Institute (H.S. Malik). D.B. Stetson is a scholar of the Rita Allen Foundation.

The authors declare no competing financial interests.

Author contributions: R.L. Brunette performed most of the experiments, analyzed the data, and helped write the manuscript. J.M. Young and H.S. Malik performed the bioinformatic and phylogenetic analyses of mammalian ALR genes and helped write the manuscript. D.G. Whitley generated expression and siRNA vectors, validated QPCR primers, and tested ALR knockdowns. I.E. Brodsky generated the inflammasome reporter cells and provided input on experiments. D.B. Stetson conceived the research project, supervised the work, and helped write the manuscript.

Submitted: 31 August 2012
Accepted: 26 September 2012

REFERENCES

Ablasser, A., F. Bauernfeind, G. Hartmann, E. Latz, K.A. Fitzgerald, and V. Hornung. 2009. RIG-I-dependent sensing of poly(dA:dT) through the induction of an RNA polymerase III-transcribed RNA intermediate. *Nat. Immunol.* 10:1065–1072. http://dx.doi.org/10.1038/ni.1779

Albrecht, M., D. Choubey, and T. Lengauer. 2005. The HIN domain of IFI-200 proteins consists of two OB folds. *Biochem. Biophys. Res. Commun.* 327:679–687. http://dx.doi.org/10.1016/j.bbrc.2004.12.056

Barbalat, R., S.E. Ewald, M.L. Mouchess, and G.M. Barton. 2011. Nucleic acid recognition by the innate immune system. *Annu. Rev. Immunol.* 29:185–214. http://dx.doi.org/10.1146/annurev-immunol-031210-101340

Bürckstümmer, T., C. Baumann, S. Blüml, E. Dixit, G. Dürnberger, H. Jahn, M. Planyavsky, M. Bilban, J. Colinge, K.L. Bennett, and G. Superti-Furga. 2009. An orthogonal proteomic-genomic screen identifies AIM2 as a cytoplasmic DNA sensor for the inflammasome. *Nat. Immunol.* 10:266–272. http://dx.doi.org/10.1038/ni.1702

Burdette, D.L., K.M. Monroe, K. Sotelo-Troha, J.S. Iwig, B. Eckert, M. Hyodo, Y. Hayakawa, and R.E. Vance. 2011. STING is a direct innate immune sensor of cyclic di-GMP. *Nature.* 478:515–518. http://dx.doi.org/10.1038/nature10429

Chiu, Y.H., J.B. Macmillan, and Z.J. Chen. 2009. RNA polymerase III detects cytosolic DNA and induces type I interferons through the RIG-I pathway. *Cell.* 138:576–591. http://dx.doi.org/10.1016/j.cell.2009.06.015

Elinav, E., T. Strowig, J. Henao-Mejia, and R.A. Flavell. 2011. Regulation of the antimicrobial response by NLR proteins. *Immunity*. 34:665–679. http://dx.doi.org/10.1016/j.immuni.2011.05.007

Fernandes-Alnemri, T., J.W. Yu, P. Datta, J. Wu, and E.S. Alnemri. 2009. AIM2 activates the inflammasome and cell death in response to cytoplasmic DNA. *Nature*. 458:509–513. http://dx.doi.org/10.1038/nature07710

Fernandes-Alnemri, T., J.W. Yu, C. Juliana, L. Solorzano, S. Kang, J. Wu, P. Datta, M. McCormick, L. Huang, E. McDermott, et al. 2010. The AIM2 inflammasome is critical for innate immunity to Francisella tularensis. *Nat. Immunol.* 11:385–393. http://dx.doi.org/10.1038/ni.1859

Gall, A., P. Treuting, K.B. Elkon, Y.M. Loo, M. Gale Jr., G.N. Barber, and D.B. Stetson. 2012. Autoimmunity initiates in nonhematopoietic cells and progresses via lymphocytes in an interferon-dependent autoimmune disease. *Immunity*. 36:120–131. http://dx.doi.org/10.1016/j.immuni.2011.11.018

Harris, R.S., and M.T. Liddament. 2004. Retroviral restriction by APOBEC proteins. *Nat. Rev. Immunol.* 4:868–877. http://dx.doi.org/10.1038/nri1489

Hornung, V., and E. Latz. 2010. Intracellular DNA recognition. *Nat. Rev. Immunol.* 10:123–130. http://dx.doi.org/10.1038/nri2690

Hornung, V., A. Ablasser, M. Charrel-Dennis, F. Bauernfeind, G. Horvath, D.R. Caffrey, E. Latz, and K.A. Fitzgerald. 2009. AIM2 recognizes cytosolic dsDNA and forms a caspase-1-activating inflammasome with ASC. *Nature*. 458:514–518. http://dx.doi.org/10.1038/nature07725

Huson, D.H., D.C. Richter, C. Rausch, T. Dezulian, M. Franz, and R. Rupp. 2007. Dendroscope: An interactive viewer for large phylogenetic trees. *BMC Bioinformatics*. 8:460. http://dx.doi.org/10.1186/1471-2105-8-460

Ishii, K.J., C. Coban, H. Kato, K. Takahashi, Y. Torii, F. Takeshita, H. Ludwig, G. Sutter, K. Suzuki, H. Hemmi, et al. 2006. A Toll-like receptor-independent antiviral response induced by double-stranded B-form DNA. *Nat. Immunol.* 7:40–48. http://dx.doi.org/10.1038/ni1282

Ishii, K.J., T. Kawagoe, S. Koyama, K. Matsui, H. Kumar, T. Kawai, S. Uematsu, O. Takeuchi, F. Takeshita, C. Coban, and S. Akira. 2008. TANK-binding kinase-1 delineates innate and adaptive immune responses to DNA vaccines. *Nature*. 451:725–729. http://dx.doi.org/10.1038/nature06537

Ishikawa, H., and G.N. Barber. 2008. STING is an endoplasmic reticulum adaptor that facilitates innate immune signalling. *Nature*. 455:674–678. http://dx.doi.org/10.1038/nature07317

Ishikawa, H., Z. Ma, and G.N. Barber. 2009. STING regulates intracellular DNA-mediated, type I interferon-dependent innate immunity. *Nature*. 461:788–792. http://dx.doi.org/10.1038/nature08476

Jones, J.W., N. Kayagaki, P. Broz, T. Henry, K. Newton, K. O'Rourke, S. Chan, J. Dong, Y. Qu, M. Roose-Girma, et al. 2010. Absent in melanoma 2 is required for innate immune recognition of Francisella tularensis. *Proc. Natl. Acad. Sci. USA*. 107:9771–9776. http://dx.doi.org/10.1073/pnas.1003738107

Kato, H., O. Takeuchi, E. Mikamo-Satoh, R. Hirai, T. Kawai, K. Matsushita, A. Hiiragi, T.S. Dermody, T. Fujita, and S. Akira. 2008. Length-dependent recognition of double-stranded ribonucleic acids by retinoic acid-inducible gene-I and melanoma differentiation-associated gene 5. *J. Exp. Med.* 205:1601–1610. http://dx.doi.org/10.1084/jem.20080091

Kato, H., K. Takahasi, and T. Fujita. 2011. RIG-I-like receptors: cytoplasmic sensors for non-self RNA. *Immunol. Rev.* 243:91–98. http://dx.doi.org/10.1111/j.1600-065X.2011.01052.x

Kawai, T., K. Takahashi, S. Sato, C. Coban, H. Kumar, H. Kato, K.J. Ishii, O. Takeuchi, and S. Akira. 2005. IPS-1, an adaptor triggering RIG-I- and Mda5-mediated type I interferon induction. *Nat. Immunol.* 6:981–988. http://dx.doi.org/10.1038/ni1243

Kent, W.J., C.W. Sugnet, T.S. Furey, K.M. Roskin, T.H. Pringle, A.M. Zahler, and D. Haussler. 2002. The human genome browser at UCSC. *Genome Res.* 12:996–1006.

Kerur, N., M.V. Veettil, N. Sharma-Walia, V. Bottero, S. Sadagopan, P. Otageri, and B. Chandran. 2011. IFI16 acts as a nuclear pathogen sensor to induce the inflammasome in response to Kaposi Sarcoma-associated herpesvirus infection. *Cell Host Microbe*. 9:363–375. http://dx.doi.org/10.1016/j.chom.2011.04.008

Kim, B.H., A.R. Shenoy, P. Kumar, R. Das, S. Tiwari, and J.D. MacMicking. 2011. A family of IFN-γ-inducible 65-kD GTPases protects against bacterial infection. *Science*. 332:717–721. http://dx.doi.org/10.1126/science.1201711

Kingsmore, S.F., J. Snoddy, D. Choubey, P. Lengyel, and M.F. Seldin. 1989. Physical mapping of a family of interferon-activated genes, serum amyloid P-component, and alpha-spectrin on mouse chromosome 1. *Immunogenetics*. 30:169–174. http://dx.doi.org/10.1007/BF02421202

McWhirter, S.M., R. Barbalat, K.M. Monroe, M.F. Fontana, M. Hyodo, N.T. Joncker, K.J. Ishii, S. Akira, M. Colonna, Z.J. Chen, et al. 2009. A host type I interferon response is induced by cytosolic sensing of the bacterial second messenger cyclic-di-GMP. *J. Exp. Med.* 206:1899–1911. http://dx.doi.org/10.1084/jem.20082874

Meredith, R.W., J.E. Janečka, J. Gatesy, O.A. Ryder, C.A. Fisher, E.C. Teeling, A. Goodbla, E. Eizirik, T.L. Simão, T. Stadler, et al. 2011. Impacts of the Cretaceous Terrestrial Revolution and KPg extinction on mammal diversification. *Science*. 334:521–524. http://dx.doi.org/10.1126/science.1211028

Muruve, D.A., V. Pétrilli, A.K. Zaiss, L.R. White, S.A. Clark, P.J. Ross, R.J. Parks, and J. Tschopp. 2008. The inflammasome recognizes cytosolic microbial and host DNA and triggers an innate immune response. *Nature*. 452:103–107. http://dx.doi.org/10.1038/nature06664

Opdenakker, G., J. Snoddy, D. Choubey, E. Toniato, D.D. Pravtcheva, M.F. Seldin, F.H. Ruddle, and P. Lengyel. 1989. Interferons as gene activators: a cluster of six interferon-activatable genes is linked to the erythroid alpha-spectrin locus on murine chromosome 1. *Virology*. 171:568–578. http://dx.doi.org/10.1016/0042-6822(89)90626-0

Punta, M., P.C. Coggill, R.Y. Eberhardt, J. Mistry, J. Tate, C. Boursnell, N. Pang, K. Forslund, G. Ceric, J. Clements, et al. 2012. The Pfam protein families database. *Nucleic Acids Res.* 40(Database issue):D290–D301. http://dx.doi.org/10.1093/nar/gkr1065

Rathinam, V.A., Z. Jiang, S.N. Waggoner, S. Sharma, L.E. Cole, L. Waggoner, S.K. Vanaja, B.G. Monks, S. Ganesan, E. Latz, et al. 2010. The AIM2 inflammasome is essential for host defense against cytosolic bacteria and DNA viruses. *Nat. Immunol.* 11:395–402. http://dx.doi.org/10.1038/ni.1864

Roberts, Z.J., N. Goutagny, P.Y. Perera, H. Kato, H. Kumar, T. Kawai, S. Akira, R. Savan, D. van Echo, K.A. Fitzgerald, et al. 2007. The chemotherapeutic agent DMXAA potently and specifically activates the TBK1-IRF-3 signaling axis. *J. Exp. Med.* 204:1559–1569. http://dx.doi.org/10.1084/jem.20061845

Roberts, T.L., A. Idris, J.A. Dunn, G.M. Kelly, C.M. Burnton, S. Hodgson, L.L. Hardy, V. Garceau, M.J. Sweet, I.L. Ross, et al. 2009. HIN-200 proteins regulate caspase activation in response to foreign cytoplasmic DNA. *Science*. 323:1057–1060. http://dx.doi.org/10.1126/science.1169841

Rozzo, S.J., J.D. Allard, D. Choubey, T.J. Vyse, S. Izui, G. Peltz, and B.L. Kotzin. 2001. Evidence for an interferon-inducible gene, Ifi202, in the susceptibility to systemic lupus. *Immunity*. 15:435–443. http://dx.doi.org/10.1016/S1074-7613(01)00196-0

Saito, T., D.M. Owen, F. Jiang, J. Marcotrigiano, and M. Gale Jr. 2008. Innate immunity induced by composition-dependent RIG-I recognition of hepatitis C virus RNA. *Nature*. 454:523–527. http://dx.doi.org/10.1038/nature07106

Sauer, J.D., K. Sotelo-Troha, J. von Moltke, K.M. Monroe, C.S. Rae, S.W. Brubaker, M. Hyodo, Y. Hayakawa, J.J. Woodward, D.A. Portnoy, and R.E. Vance. 2011. The N-ethyl-N-nitrosourea-induced Goldenticket mouse mutant reveals an essential function of Sting in the in vivo interferon response to *Listeria monocytogenes* and cyclic dinucleotides. *Infect. Immun.* 79:688–694. http://dx.doi.org/10.1128/IAI.00999-10

Schattgen, S.A., and K.A. Fitzgerald. 2011. The PYHIN protein family as mediators of host defenses. *Immunol. Rev.* 243:109–118. http://dx.doi.org/10.1111/j.1600-065X.2011.01053.x

Seth, R.B., L. Sun, C.K. Ea, and Z.J. Chen. 2005. Identification and characterization of MAVS, a mitochondrial antiviral signaling protein that activates NF-kappaB and IRF 3. *Cell*. 122:669–682. http://dx.doi.org/10.1016/j.cell.2005.08.012

Sharma, S., R.B. DeOliveira, P. Kalantari, P. Parroche, N. Goutagny, Z. Jiang, J. Chan, D.C. Bartholomeu, F. Lauw, J.P. Hall, et al. 2011.

Innate immune recognition of an AT-rich stem-loop DNA motif in the Plasmodium falciparum genome. *Immunity*. 35:194–207. http://dx.doi.org/10.1016/j.immuni.2011.05.016

Stajich, J.E., D. Block, K. Boulez, S.E. Brenner, S.A. Chervitz, C. Dagdigian, G. Fuellen, J.G. Gilbert, I. Korf, H. Lapp, et al. 2002. The Bioperl toolkit: Perl modules for the life sciences. *Genome Res*. 12:1611–1618. http://dx.doi.org/10.1101/gr.361602

Stetson, D.B., and R. Medzhitov. 2006. Recognition of cytosolic DNA activates an IRF3-dependent innate immune response. *Immunity*. 24:93–103. http://dx.doi.org/10.1016/j.immuni.2005.12.003

Stetson, D.B., J.S. Ko, T. Heidmann, and R. Medzhitov. 2008. Trex1 prevents cell-intrinsic initiation of autoimmunity. *Cell*. 134:587–598. http://dx.doi.org/10.1016/j.cell.2008.06.032

Strowig, T., J. Henao-Mejia, E. Elinav, and R. Flavell. 2012. Inflammasomes in health and disease. *Nature*. 481:278–286. http://dx.doi.org/10.1038/nature10759

Takaoka, A., Z. Wang, M.K. Choi, H. Yanai, H. Negishi, T. Ban, Y. Lu, M. Miyagishi, T. Kodama, K. Honda, et al. 2007. DAI (DLM-1/ZBP1) is a cytosolic DNA sensor and an activator of innate immune response. *Nature*. 448:501–505. http://dx.doi.org/10.1038/nature06013

Torgerson, D.G., E.J. Ampleford, G.Y. Chiu, W.J. Gauderman, C.R. Gignoux, P.E. Graves, B.E. Himes, A.M. Levin, R.A. Mathias, D.B. Hancock, et al; Mexico City Childhood Asthma Study (MCAAS); Children's Health Study (CHS) and HARBORS study; Genetics of Asthma in Latino Americans (GALA) Study, Study of Genes-Environment and Admixture in Latino Americans (GALA2) and Study of African Americans, Asthma, Genes & Environments (SAGE); Childhood Asthma Research and Education (CARE) Network; Childhood Asthma Management Program (CAMP); Study of Asthma Phenotypes and Pharmacogenomic Interactions by Race-Ethnicity (SAPPHIRE); Genetic Research on Asthma in African Diaspora (GRAAD) Study. 2011. Meta-analysis of genome-wide association studies of asthma in ethnically diverse North American populations. *Nat. Genet*. 43:887–892. http://dx.doi.org/10.1038/ng.888

Unterholzner, L., S.E. Keating, M. Baran, K.A. Horan, S.B. Jensen, S. Sharma, C.M. Sirois, T. Jin, E. Latz, T.S. Xiao, et al. 2010. IFI16 is an innate immune sensor for intracellular DNA. *Nat. Immunol*. 11:997–1004. http://dx.doi.org/10.1038/ni.1932

Yan, N., A.D. Regalado-Magdos, B. Stiggelbout, M.A. Lee-Kirsch, and J. Lieberman. 2010. The cytosolic exonuclease TREX1 inhibits the innate immune response to human immunodeficiency virus type 1. *Nat. Immunol*. 11:1005–1013. http://dx.doi.org/10.1038/ni.1941

Yoneyama, M., M. Kikuchi, T. Natsukawa, N. Shinobu, T. Imaizumi, M. Miyagishi, K. Taira, S. Akira, and T. Fujita. 2004. The RNA helicase RIG-I has an essential function in double-stranded RNA-induced innate antiviral responses. *Nat. Immunol*. 5:730–737. http://dx.doi.org/10.1038/ni1087

Young, J.M., C. Friedman, E.M. Williams, J.A. Ross, L. Tonnes-Priddy, and B.J. Trask. 2002. Different evolutionary processes shaped the mouse and human olfactory receptor gene families. *Hum. Mol. Genet*. 11:535–546. http://dx.doi.org/10.1093/hmg/11.5.535

Zhang, Z., B. Yuan, M. Bao, N. Lu, T. Kim, and Y.J. Liu. 2011. The helicase DDX41 senses intracellular DNA mediated by the adaptor STING in dendritic cells. *Nat. Immunol*. 12:959–965. http://dx.doi.org/10.1038/ni.2091